SUPPORTING INFORMATION

A Microneedle with Photoactive Electrospun Backing Layer Enables Multitherapy and Combined Drug Delivery to the Skin Wound

Maryam Toolabi[1,2,3], Yuewen Zhu[4], Mahsa Akbari[1,2], Mohammad Reza Eskandari[3], Narges Forouzideh[1], Hélder A. Santos[4,*], Mohammad-Ali Shahbazi[4,*]

[1] Department of Pharmaceutical Nanotechnology, School of Pharmacy, Zanjan University of Medical Sciences, 45139-56184 Zanjan, Iran

[2] Zanjan Pharmaceutical Nanotechnology Center, Zanjan University of Medical Sciences, Zanjan, Iran

[3] Department of Pharmacology and Toxicology, School of Pharmacy, Zanjan University of Medical Science, 45139-56184 Zanjan, Iran

[4] Department of Biomaterials and Biomedical Technology, The Personalized Medicine Research Institute (PRECISION), University Medical Center Groningen (UMCG), University of Groningen, Antonius Deusinglaan 1, 9713 AV, Groningen, Netherlands

*Corresponding Authors: h.a.santo@umcg.nl; m.a.shahbazi@umcg.nl

1. Experimental Section

1.1. Synthesis and Characteristics of Bi_2S_3 NRs

Bi_2S_3 NRs were synthesized by a simple chemical method.[1] In a typical synthesis, 90 mg polyvinylpyrrolidone (PVP) ($(C_6H_9NO)_n$; Sigma-Aldrich, USA) was dissolved in 3 ml deionized water (DW), then 121.25 mg of bismuth nitrate pentahydrate ($Bi(NO_3)_3.5H_2O$; 98%, SAMCHUN, South Korea) was added and dissolved. In the next step, 260 mg of thioacetamide (C_2H_5NS; >98%, Merck, Germany) was dissolved in 2 ml of DW and added to the mixture of PVP and bismuth nitrate pentahydrate while stirring. The pH of the reaction mixture was adjusted to 0.5 by adding hydrochloric acid (HCl) solution and stirring at 50 °C for 4 h. After the end of the reaction, the formation of a black-brown precipitate indicates the synthesis of Bi_2S_3 NRs. The synthesized Bi_2S_3 NRs were then collected using centrifugation at 13,000 rpm for 10 min, washed three times with DW, and stored at 4 °C for further use.

The morphology and size of Bi_2S_3 NRs were investigated by transmission electron microscopy (TEM) (Philips EM 208S, Netherlands), operating at an accelerating voltage of 100 kV. Zeta potential measurement was determined via dynamic light scattering (DLS) analysis using a Horiba Scientific Nanoparticle size analyzer (SZ-100, Malvern, UK) at room temperature. Elemental analysis of Bi_2S_3 NRs was performed using energy-dispersive X-ray spectrometry (EDX) (Bruker Nano GmbH, Berlin, Germany). The NIR absorbance spectra of Bi_2S_3 NRs were recorded in the range of 700 to 900 nm by a spectrophotometer (Genesys 10-S, USA).

1.2. *In vitro* Photothermal Performance

To investigate the photothermal performance of the Bi_2S_3 NRs, 1 ml aqueous dispersion of Bi_2S_3 NRs with concentrations of 50, 100, and 200 μg ml^{-1} was irradiated under 808 nm NIR laser (0.5, 1.0, and 1.5 W cm^{-2}) for 10 min. The temperature change was recorded at 1 min intervals by an

infrared thermal camera. The photothermal stability of Bi_2S_3 NRs was evaluated by repeating five cycles of 808 nm laser irradiation (1.5 W cm^{-2}, 10 min) for a concentration of 200 μg ml^{-1}, followed by a cooling phase of 15 min for each cycle.

1.3. Photothermal Conversion Efficiency

To calculate the photothermal conversion efficiency (η), 1 ml of the aqueous dispersion of Bi_2S_3 NRs (200 μg ml^{-1}) was irradiated with an 808 nm laser (1.5 W cm^{-2}) for 10 min. Then the laser was turned off, and the temperature was recorded every 30 s in the cooling phase. The η value for Bi_2S_3 NRs was quantified by the following Eq. (1):

$$\eta = \frac{hA(T_{max} - T_{surr}) - Q_{dis}}{I - (1 - 10^{-A_{808}})} \qquad (1)$$

Where h is the heat transfer coefficient. A is the surface area of the container. T_{max} and T_{surr} are the maximum steady-state temperature (50.4 °C) for the Bi_2S_3 NRs solution and the surrounding temperature (27.9 °C), respectively. Q_{dis} is the heat loss associated with light absorbance by the solvent and container. I indicate the laser power density (1.5 W cm^{-2}). A_{808} is the absorbance of the Bi_2S_3 NRs (200 μg ml^{-1}) at 808 nm (0.83). The value of hA was obtained from Eq. (2):

$$hA = \frac{m_d c_d}{\tau_s} \qquad (2)$$

Then, using Eq. (3), the time constant (τ_s) of the Bi_2S_3 NRs was obtained:

$$\tau_s = \frac{t}{-ln\theta} \qquad (3)$$

and θ was calculated using Eq. (4):

$$\theta = \frac{\Delta T}{\Delta T_{max}} \qquad (4)$$

ΔT is the difference between the temperature of the Bi_2S_3 NRs and the environment at any time.

As shown in Fig. 1l, τ_s (277.65) was calculated by plotting the time data in the cooling phase of Fig. 1k *versus* -ln(θ).

Thus, the hA value was obtained from Eq. (2). m_d and c_d are the mass (1.0 g) and heat capacity (4.2 J g^{-1} $°C^{-1}$) of the DW in aqueous dispersion of Bi_2S_3 NRs, respectively. Therefore, the hA was calculated to be 15 mW $°C^{-1}$.

Q_{dis}, which is heat loss by DW and container, was calculated based on Eq. (5):

$$Q_{dis} = \frac{m_d c_d \Delta T_{DW}}{\tau_s} \qquad (5)$$

where, the m_d is the mass of 1 g of DW irradiated with an 808 nm laser (1.5 W cm^{-2}) for 10 min, and ΔT_{DW}, the difference between the maximum DW temperature after laser light irradiation and the ambient temperature, was measured to be 7 °C.

Then the value of τ_s was calculated as 213.82. Therefore, Q_{dis} was calculated to be 137 mW.

In addition, the η value of the Bi_2S_3 NRs loaded in PGTBi nanofibrous scaffolds was calculated to be 15.7, according to Eq. (1).

1.4. Fabrication of Tau and Bi_2S_3 NRs loaded PVA/Gela Nanofibrous Scaffolds

1.4.1. Preparation of Electrospinning Solution

Initially, poly (vinyl alcohol) (PVA; Sigma-Aldrich, USA; Mw 85000-124000; 99+% hydrolyzed) and gelatin (Gela; porcine skin gel strength 300; Type A; Sigma-Aldrich) solutions were prepared, independently. A 10% w/v PVA solution was prepared by dissolving PVA powder in DW at about 90 °C with constant stirring for 6 h. The solution of 8% w/v Gela was prepared by dissolving Gela powder in a 30% v/v acetic acid solution at 50 °C under gentle stirring for 1 h. Various blend solutions of PVA/Gela (PG), PVA/Gela/Bi_2S_3 NRs (PGBi), PVA/Gela/Taurine(Tau) (PGT), and PVA/Gela/Tau/Bi_2S_3 NRs (PGTBi) were prepared. At first, to prepare the PG solution, PVA and Gela solutions were mixed at a 7:3 volume ratio and stirred overnight at room temperature. To

prepare the PGBi solution, after mixing the PVA and Gela solution for 1 h, Bi_2S_3 NRs (200 µg ml^{-1}) were added and stirred overnight at room temperature. PGTBi and PGT solutions were prepared by adding Tau powder (5% w/v; Sigma-Aldrich; USA) to PGBi and PG solutions, respectively, and stirred for 2 h at room temperature. The taurine concentration (5% w/v) used in the electrospinning solution was determined through comprehensive preliminary tests aimed at optimizing solution process ability, fiber morphology, and functional performance. Different taurine concentrations were initially evaluated, and 5% w/v was selected as it provided stable electrospinning, uniform bead-free nanofibers, and acceptable mechanical integrity, while higher concentrations led to jet instability and fiber defects. Previous studies have indicated that 5% w/v Tau was chosen as the optimum concentration for in vivo study on the full-thickness excisional wounds.[2, 3]

1.4.2. Electrospinning

The nanofibrous scaffolds were prepared using electrospinning equipment at room temperature. The electrospinning solutions were loaded into a 5 ml syringe with a 22 G needle and set up in the electrospinning apparatus (Electroris ES-100 instrument, Fnm Co, IR). The applied voltage was fixed at 24 kV, and the distance between the needle tip and the collector was determined to be 15 cm. The solution was injected from the syringe at a flow rate of 0.5 ml h^{-1}. The nanofibrous scaffolds were collected on an aluminum foil attached to a collector with a rotation speed of 200-220 rpm. Then, the nanofibrous scaffolds were heated at 150 °C for 1 h to induce cross-linking.

1.5. Fabrication of Microneedle Patches

The PGTBi-PHA microneedle (MN) patches were fabricated via a molding method in a two-step casting process. Poly(methyl vinyl ether-alt-maleic anhydride) (PMVE-MA; 20% w/v; Sigma-Aldrich; USA; Mw 1,080,000 Da), hyaluronic acid (HA; 0.5% w/v; High molecular weight;

Bloomage Biotechnology Corp., Ltd., China), and allantoin (Alla, 0.5% w/v; ≥98%; Sigma-Aldrich; USA) were dissolved together in DW to prepare the pre-gel solution of MN needles (PHA). 300 µl of PHA pre-gel solution was added to the polydimethylsiloxane (PDMS) mold (height: 800 µm, base width: 200 µm; Singapore) and the mold was centrifuged at 4,500 rpm for 20 min to fill the microcavities. Next, the nanofiber scaffolds were cut to the size of the mold backing layer, placed on the mold, and dried in a desiccator at room temperature for 48 h. Finally, the PGTBi-PHA MN patches were gently peeled out of the molds and stored in the desiccator containing silica gel for further use.

1.6. Characterization of MN Patches

1.6.1. Morphology

The surface morphology of the electrospun nanofibers was observed using scanning electron microscopy (SEM VEGA3, TESCAN, Czech Republic) at an acceleration voltage of 10 kV. Samples were gold sputter-coated before viewing to minimize charging effects. The obtained images were analyzed using Image J software to determine the diameter of the nanofibers. The average diameter and size distribution of nanofibers were calculated from 100 random measurements per image. The morphology of MN patches was investigated by SEM.

1.6.2. FTIR, XRD, EDX, TGA, and DTG Analysis

The chemical structure of the nanofibrous scaffolds and MN needles was determined using a Fourier transform infrared (FTIR) spectrometer (Bruker, Germany). All spectra were recorded in the wavelength range of 4000 to 500 cm^{-1} at room temperature. The crystalline nature of pure components, Bi_2S_3 NRs, nanofibrous scaffolds, and MN needles was analyzed using X-ray diffraction (XRD, PW 1730, Philips, Netherlands) at room temperature with a 2θ angle range of 10 to 80 °θ at a rate of 0.05 °θ s^{-1}. Elemental analysis of the nanofibrous scaffolds and needles of

MN was performed using EDX spectroscopy (Bruker Nano GmbH, Berlin, Germany). The thermal behavior of nanofibrous scaffolds and their ingredients was analyzed by the thermogravimetric analysis (TGA, SDT-Q600, USA) and differential thermogravimetric analysis (DTG) in the heating temperature range from 30 to 800 °C with a controlled heating rate of 10 °C min^{-1} under argon atmosphere.

1.7. *In vitro* Degradation of Nanofibrous Scaffolds

To perform degradation studies, the nanofiber scaffolds were first cut into 2 × 2 cm^2 pieces. The initial weight (W_1) of each was measured, and the samples were incubated in 5 ml of phosphate-buffered saline (PBS, pH 7.4) at 37 °C for 1, 2, 3, and 4 h. Then, the samples were removed from PBS, washed three times with fresh PBS, and dried in an oven at 37 °C overnight. After complete dehydration, the weight of the dried samples (W_2) was measured, and the relative weight loss was calculated using the following Eq. (6):

$$Weight\ loss\ (\%) = \frac{(W_1 - W_2)}{W_1} \times 100 \qquad (6)$$

.

1.8. Mechanical Properties of the Nanofibrous Scaffolds

The mechanical properties of the nanofiber scaffolds were determined using a mechanical testing machine (SANTAM-STM5). The selected samples with different thicknesses were cut into 30 mm (length) × 20 mm (width) sizes, and the thickness of the fibrous membranes was measured using a digital micrometer. The samples were mounted vertically on the gripping unit of the tensile tester with a cross-head speed of 5 mm min^{-1}. Young's modulus (MPa), break strength (BS), and ultimate tensile strength (UTS) of the nanofiber scaffolds were calculated using the slope of the stress-strain curves, Eq. (7 and 8), respectively:

$$BS = \frac{L_{max}}{L_0} \times 100 \qquad (7)$$

$$UTS = \frac{F_{max}}{A} \qquad (8)$$

where, L_0 is the length of the sample, L_{max} is the maximum length at the breaking point, F_{max} is the input load at the breaking point of the sample, and A is the cross-sectional area of the samples.

1.9. Water Contact Angle of the Nanofibrous Scaffolds

The wettability of nanofiber scaffolds was evaluated by measuring the contact angle of a water droplet with the nanofiber surface using a static contact angle measuring instrument (Contact Angle CAG-20). Three samples of each nanofibrous scaffold were investigated for average contact angle.

1.10. Mechanical and Insertion Characterization of MN patches

The mechanical strength of the microneedle patches was examined using a texture analyzer. The MN patches were fixed on a piece of stainless steel with the tips of the needles facing upwards. Then, the sensor approached the tips of the needles at a speed of 0.2 mm s^{-1} in the vertical direction, and the compression force was recorded as a function of displacement.

Parafilm M®, a flexible thermoplastic polymer film, was used as a previously validated skin simulant to evaluate the insertion capability of MN patches.[4, 5] Eight layers of Parafilm M® were cut into 2 × 2 cm^2 dimensions and were stacked to create a skin model with an approximate thickness of 1 mm. The MN patches were applied to the Parafilm M® layers with a spring applicator for 1 min. Three replicates were performed for each sample. Then, the MN patches were carefully separated from the Parafilm M® layers after insertion. To assess the penetration depth of MN patches, the Parafilm M® layers were separated and imaged using a high-resolution mobile phone (Samsung A72). The number of holes made in each layer by the MN patches was counted. The penetration percentage of MN patches was calculated using the following Eq. (9):[6]

$$The\ penetration\ percentage\ of\ MN\ patche = \frac{Number\ of\ holes\ per\ each\ layer}{Number\ of\ needles\ per\ MN\ patche} \times 100 \qquad (9)$$

To evaluate the skin penetration ability, MN patches loaded with 4% trypan blue were applied to the skin of a hairless rat cadaver using an applicator for 1 min and then removed. After that, images of the microchannels created on the skin were taken using a high-resolution mobile phone (Samsung A72).

1.11. *In vitro* and *In vivo* Dissolution of MN Patches

In vitro dissolution of PHA and PGTBi-PHA MN patches was investigated using PBS solution (pH 7.4). MN patches were placed in PBS solution and then imaged using a high-resolution mobile phone (Samsung A72) at 0, 15, 20, 25, and 45 min.

In vivo dissolution of PH, PHA, PGTBi-PH, and PGTBi-PHA MN patches was evaluated in the wound created on the back skin of a rat. MN patches were inserted into the wound with an applicator and then removed from the wound surface after 1, 3, 5, and 10 min post-insertion. Length changes of the treated MN patches were observed using field emission scanning electron microscopy (FESEM).

1.12. Biocompatibility of MN Patches

1.12.1. Hemocompatibility of MN Patches

A hemolysis assay was carried out to investigate the effect of MN patches on red blood cells (RBCs). To perform the hemolysis test, 10 ml of anti-coagulated human blood was first taken from a healthy volunteer and poured into 50 ml falcon. To separate the RBCs, twice the blood volume of PBS (pH 7.4) was slowly added to the blood and centrifuged at 3000 rpm for 6 min. After the centrifuge, the white supernatant was discarded and again twice the volume of blood of PBS was added to it and centrifuged at 3000 rpm for 6 min. This protocol was repeated 5 times to create a pure RBC at the bottom of the falcon. Then, 1 ml of pure RBC was added to 19 ml of PBS to make a 5% hematocrit concentration. The nanofiber scaffolds were cut in weights of 1, 2, 4, and 8 mg,

each with 3 replicates. Nanofiber samples were placed in 2 ml microtubes, and 0.8 ml of PBS was added to each microtube. Then 0.2 ml of 5% hematocrit was added to each of these microtubes and incubated for 1, 4, 8, and 24 h. After incubation, the microtubes were centrifuged at 6000 rpm for 5 min, and then 150 µl of the supernatant was removed from each microtube and placed inside a 96-well plate. Then the absorbance was read at 540 nm with an ELISA reader (infinite M200, Austria). Hemolysis assay of PH and PHA MN needles was also done using the same method, with the difference that the freeze-dried needles were dispersed in PBS at different concentrations. Then, 0.8 ml of suspension was mixed with 0.2 ml of 5% hematocrit to reach the final concentrations of 50, 100, 200, and 400 µg ml^{-1} of PH and PHA in a 2 ml microtubes and incubated for 1, 4, 8, 24, and 48 h. The percentage of non-hemolyzed RBC of each sample was calculated using Eq. (10):

$$Non-\ Hemolyzed\ RBCs\ (\%) = \left[100 - \left(\frac{(A_s - A_n)}{(A_p - A_n)} \times 100\right)\right] \qquad (10)$$

where, A_s is the sample absorbance, A_n is the absorbance of the negative control, and A_p is the absorbance of the positive control. In this assay, fresh PBS buffer (pH 7.4) and DW were used as the negative and positive control, respectively.

1.12.2. *In vitro* Cytocompatibility of MN Patches

The biocompatibility of PG, PGT, PGBi, and PGTBi nanofibrous scaffolds and MN needles of PH and PHA was evaluated by co-culturing them with the L929 mouse fibroblast cell line. L929 cells were cultured in minimum essential medium (MEM) supplemented with 10% (v/v) fetal bovine serum (FBS), 1% (v/v) penicillin/streptomycin, and 1% (v/v) GlutaMAX (All cell culture products were sourced from Gibco, Thermo Fisher Scientific Inc). The cultured cells were incubated in a humidified incubator at 37 °C with 5% CO_2. When the cells reached 70 - 80% confluency, they were subcultured. Before cell seeding, the PG, PGT, PGBi, and PGTBi nanofibrous scaffolds were

cut into a square of about 0.8 × 0.8 cm, and sterilized by ultraviolet (UV) irradiation for 15 min. Then the nanofibrous scaffolds were placed in a 24-well plate and 50 µl of medium was added to each well to moisten the scaffolds. Subsequently, 100 µl of cell suspension with a density of ~6×10^6 cell ml^{-1} was seeded onto the nanofibrous scaffolds, and after 5 min, 1 ml of additional medium was added along the well wall. The viability of L929 cells on nanofibrous scaffolds was assessed using the live/dead™ (green/deep red) kit (Thermo Fisher Scientific Inc.) after 4 and 11 days in culture. A confocal laser scanning microscopy (CLSM) (Stellaris 5, Leica Microsystems) was used to examine cell morphology and take images.

Cytotoxicity of the PH and PHA MN needles was determined using the CellTiter-Glo luminescent cell viability assay (Promega Corporation) according to the manufacturer's description. After L929 cells (~1×10^5 cell ml^{-1}) were seeded onto 96-well plates for 24 and 48 h, the cell culture medium was replaced by the medium containing PH and PHA with different concentrations (0.125, 0.25, 0.5, and 1 mg ml^{-1}). Cell viability was measured and analyzed by the CellTiter-Glo kit and a multimode microplate reader (Gen 5, BioTek Instruments, Inc.) after 24 and 48 h of co-incubation. The experiment was set up with 4 parallel wells.

1.13. Antibacterial Activity of the PGTBi Nanofibers

In this study, Gram-negative bacteria of *Escherichia coli* (*E. coli*) (ATCC 25922) and Gram-positive bacteria of *Staphylococcus aureus* (*S. aureus*) (ATCC 25923) were used as model bacteria to evaluate the in vitro antibacterial properties of the electrospinning solution. Both types of bacteria were cultured at 37 °C in sterilized nutrient broth in a shaking incubator at 150 rpm to prepare a 0.5 McFarland standard (1.5×10^8 CFU ml^{-1}). After that, the bacterial suspension was diluted in normal saline (0.9% w/v) to reach a concentration of 0.5×10^8 CFU ml^{-1}. Then 20 µl of diluted bacterial suspension (10^6 CFU ml^{-1} bacteria) was added to 1 ml of sterilized electrospinning

solution and normal saline as a control group. The obtained mixtures were irradiated using an NIR laser (808 nm; power density 1.5 W cm^{-2}) for 10 min and incubated at 25 °C for 2 h. The resulting mixture was then diluted 30 times by adding normal saline, and 100 µl of the diluted suspension was uniformly dispersed on agar plates and incubated at 37 °C overnight to observe the colony-forming units (CFUs). Each sample was studied in triplicate.

1.14. *In vivo* Toxicity of MN Patches

In vivo toxicity of MN patches was investigated from views of blood biochemical and histological analysis in rats (230-250 g). For this purpose, 15 male rats were randomly divided into five groups (N=3), including untreated wounds (control) and wounds treated with PG-PH, PG-PHA, PGT-PHA, and PGTBi-PHA MN patches. The animals were then anesthetized by an intraperitoneal (IP) injection of 0.25 ml of ketamine (50 mg ml^{-1})-xylazine (20 mg ml^{-1}) cocktail (6:4 v/v). Then, a full-thickness wound with a diameter of 0.9 cm was created on the back of the animals, and PG-PH, PG-PHA, PGT-PHA, and PGTBi-PHA MN patches were inserted into the wound, and the control group did not receive any treatment. After 2 weeks, fresh blood samples were collected for biochemistry and hematology monitoring. Moreover, the rats were sacrificed, and main organs such as liver, kidney, and spleen were collected and fixed in 4% formaldehyde solution overnight, followed by embedding in paraffin for H&E staining and visualization by fluorescence microscopy.

1.15. *In Vivo* Wound Healing Assessment

PGT-PHA and PGTBi-PHA MN patches were inserted into the full-thickness skin defect model of the rat to evaluate the wound healing capacity. To create the wound model, 24 male Sprague-Dawley rats (230-250 g) were randomly assigned into four groups (N=6) as follows: untreated wound (control), PGT-PHA, PGTBi-PHA, and PGTBi-PHA+NIR treated groups. After

anesthetization with IP injection of 0.25 ml of ketamine (50 mg ml^{-1})-xylazine (20 mg ml^{-1}) cocktail (6:4 v/v), the dorsal area of the rats was shaved, and 2 full-thickness circular wounds (9 mm in diameter) were produced on either backside of each rat. Then, 20 µl of S. aureus (0.5 McFarland) bacterial suspension was added to the wound bed to establish an infected wound model, and subsequently, the PGT-PHA and PGTBi-PHA MN patches were inserted into full-thickness wounds, and animals were kept separately in individual cages. Moreover, the wound site of the PGTBi-PHA+NIR treated group was irradiated by 808 nm NIR irradiation (power density of 1.5 W cm^{-2}) on days 0, 1, 2, and 3, and the wound temperature was maintained at about 40 °C for 4 min by adjusting the distance of the laser from the wound site (spot size equal to wound area) using an IR thermal imaging camera to improve wound healing. The wound healing process was photographed on days 0, 3, 7, 10, and 14, and the wound surface area in different groups was calculated using Image J software. The wound area was calculated by the following Eq. (11):

$$Wound\ area\ (\%) = \frac{A_t}{A_0} \times 100 \qquad (11)$$

where, A_0 is the wound area on day 0, and A_t is the wound area on days 3, 7, 10, and 14.

After 14 days of treatment, the rats were sacrificed, and the wound tissue samples were collected and fixed in 4% formaldehyde overnight. The skin tissue samples were then embedded in paraffin and sectioned at a thickness of 5 µm, and finally stained with H&E and Masson's trichrome to evaluate histology and visualize collagen deposition, respectively.

All in vivo assays were conducted according to the Committee of Animal Experimentation guidelines of "Zanjan University of Medical Sciences", which approved all *in vivo* procedures conducted in this study an ethical code of IR.ZUMS.REC.1400.439.

1.16. Statistical Analysis

Three replicates were performed for each sample in each experiment. Data were reported as mean ± standard deviation (SD). Statistical analyses were performed using One-way ANOVA for multiple comparisons (Tuky test) with SPSS software.

2. Results and Discussion

2.1. *In vitro* Photothermal Performance

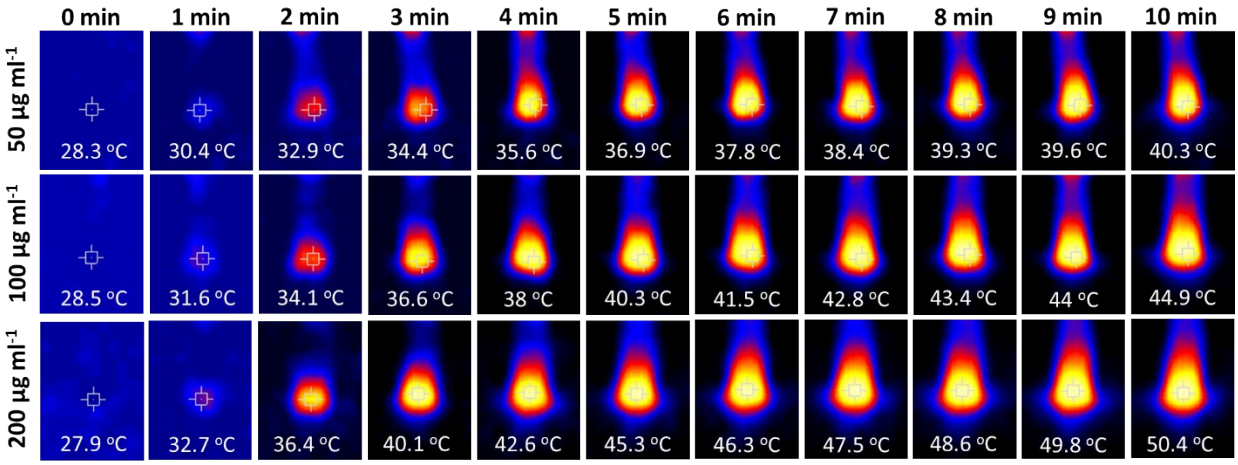

Fig. S1. Infrared thermal photographs of different concentrations (50, 100, and 200 µg ml^{-1}) of Bi_2S_3 NRs under 10 min light irradiation (808 nm) with a power density of 1.5 W cm^{-2}.

2.2. SEM images of nanofibrous scaffolds

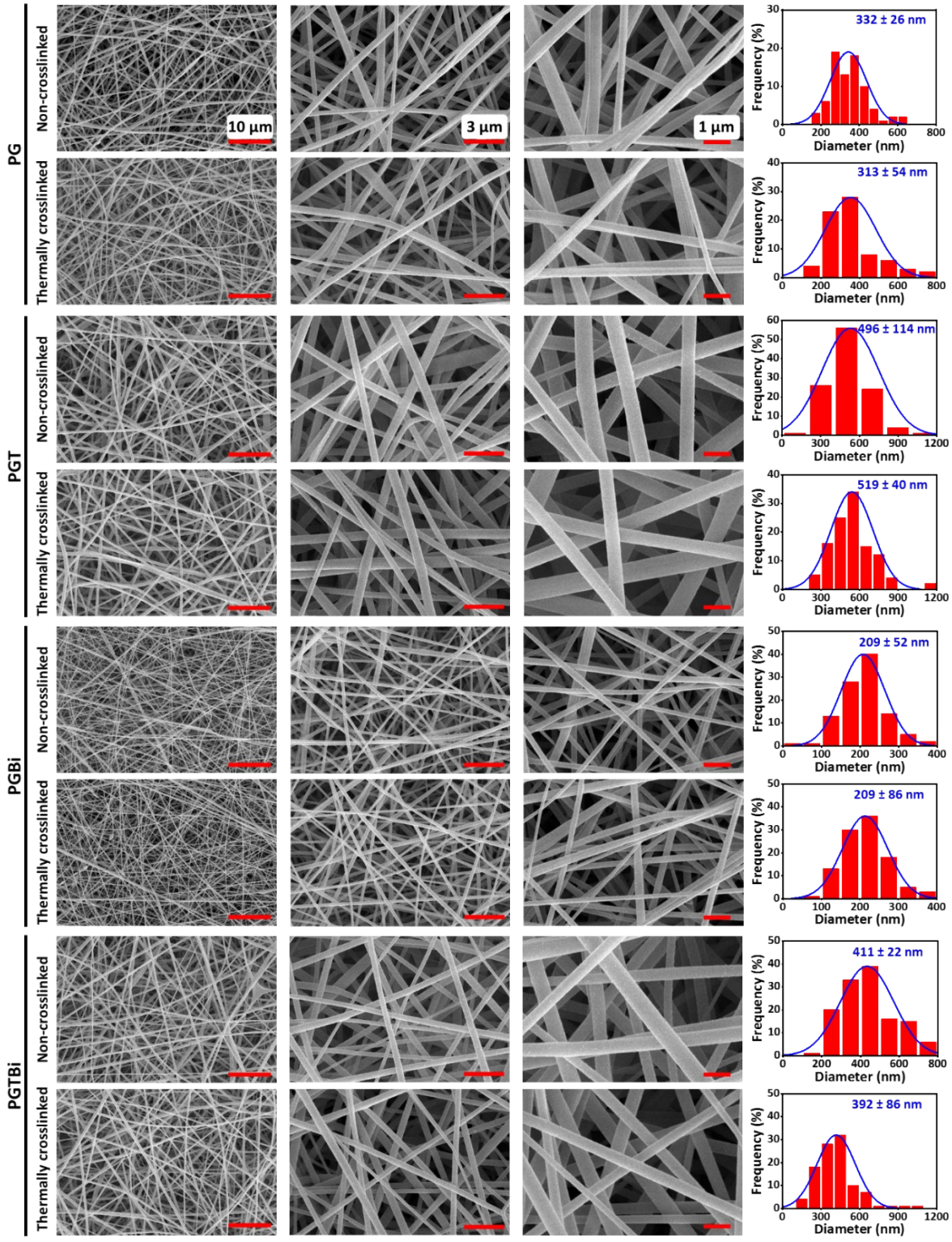

Fig. S2. SEM micrographs along with size distribution histograms of non-crosslinked and thermally crosslinked nanofibrous scaffolds of PG, PGT, PGBi, and PGTBi.

2.3. Water Contact Angle of the Nanofibrous Scaffolds

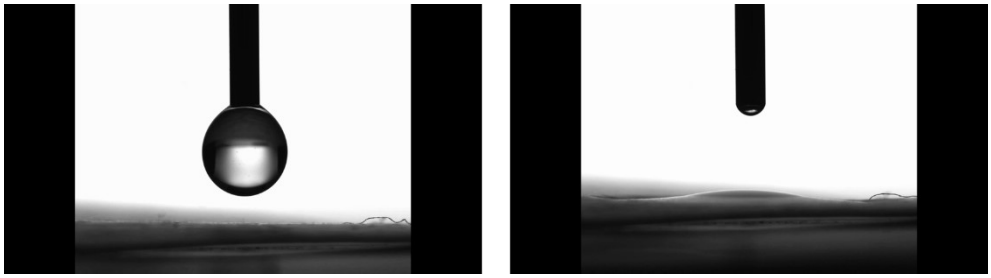

Fig. S3. Water contact angle photographs of water droplet on the surface of nanofibrous scaffolds.

2.4. EDX Analysis of Nanofibrous Scaffolds

EDX and X-ray mapping analysis of PG, PGT, PGBi, and PGTBi nanofiber scaffolds were performed to investigate the elemental analysis (Fig. S4). EDX spectra of PG and PGT nanofiber scaffolds showed the presence of C, O, and N elements in the PG nanofiber scaffolds, and C, O, N, and S elements in PGT nanofibers. The presence of Bi and S elements confirmed the existence of Bi_2S_3 NRs on the surface of PGBi and PGTBi nanofiber scaffolds. A map scanning and weight percentage of each element are shown in Fig. S4e, which shows the uniform distribution of each element on the surface of the nanofibers. These results confirmed that Bi_2S_3 NRs have a homogeneous distribution on the surface of PGBi and PGTBi nanofibers, leading to enhanced photothermal performance.

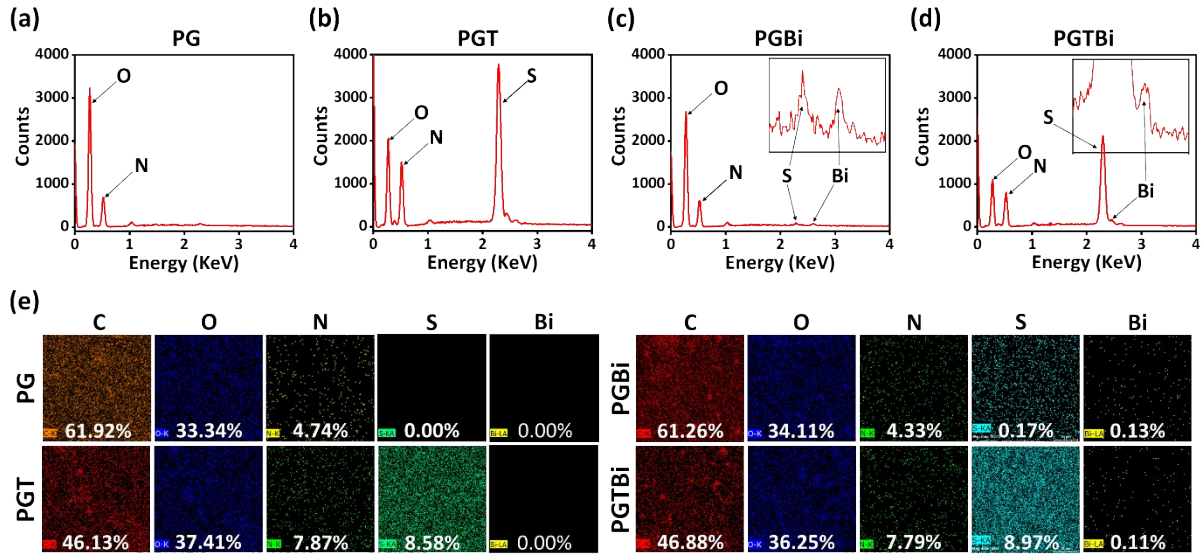

Fig. S4. EDX spectra of nanofiber scaffolds of (a) PG, (b) PGT, (c) PGBi, and (d) PGTBi. (e) X-ray mapping of PG, PGT, PGBi, and PGTBi nanofiber scaffolds**.**

2.5. TGA and DTG Analysis of Nanofibrous Scaffolds

The thermal stability of electrospun nanofibrous scaffolds was investigated by TGA and DTG curves and an analysis data table (Fig. S5). All samples except Tau demonstrated an initial weight loss step in the temperature range of 50 to 250 °C due to the loss of the absorbed moisture and solvent.[7] In addition to the initial weight loss related to moisture, PVA showed three other steps of weight loss. Major weight loss of 68.38% has occurred at 264.02 °C due to the removal of hydroxyl side groups and the release of water molecules.[8, 9] The thermal degradation of the Gela showed a maximum decomposition rate at 322.95 °C due to the breaking of the protein chain and peptide bonds, and it continued up to 800 °C, and about 18.35% ash remained.[8] The thermogram of PG nanofibers showed a 62% weight loss in the temperature range of 250 to 350 °C, which was due to the overlapping of PG components and intermolecular bonds, and a 98.92% weight loss was observed at 800 °C. Thermal degradation of Tau showed that it decomposed in two steps, the first step at 317-400 °C and the second step at 400-550 °C, which was completely decomposed due to the Tau crystalline structure. However, with the incorporation of Tau into PG, the

thermogram of PGT nanofibers shifted towards a higher temperature than the PG nanofibers thermogram, which could be attributed to enhanced intermolecular interactions between Tau and PG polymer matrices. The residual weight for PG and PGT nanofibers at 800 °C was 1.08 and 15.08%, respectively, which corresponds to the weight of carbon and ash after decomposition. Thermal analysis of Bi_2S_3 NRs showed two steps of weight loss, the first weight loss due to water loss at 150 to 250 °C, and the second weight loss due to PVP degradation at 250 to 800 °C. The remaining weight was 74.78%, which contains Bi_2S_3 NRs that were not decomposed and had high thermal stability. The thermal analysis curve of PGBi nanofibers was almost similar to that of PG nanofibers because there was a very small amount of Bi_2S_3 NRs in PGBi nanofibers. With the difference that in PGBi nanofibers, the residual weight was 5.25% at 800 °C, which was more than PG nanofibers (1.08%). In the TGA curve of PGTBi nanofibers with the presence of Tau and Bi_2S_3 NRs, the degradation temperature has increased compared to PG nanofibers, and the weight loss has reached from 98.22% in PG nanofibers to 95.25% in PGTBi nanofibers. In addition, the DTG curve of PGTBi nanofibers showed that the maximum decomposition rate of 0.83% $°C^{-1}$ occurred at 270 °C, indicating the improved thermal stability of the nanofibers. These results indicated that Tau and Bi_2S_3 NRs contribute to the thermal stability of PGTBi nanofibrous scaffolds.

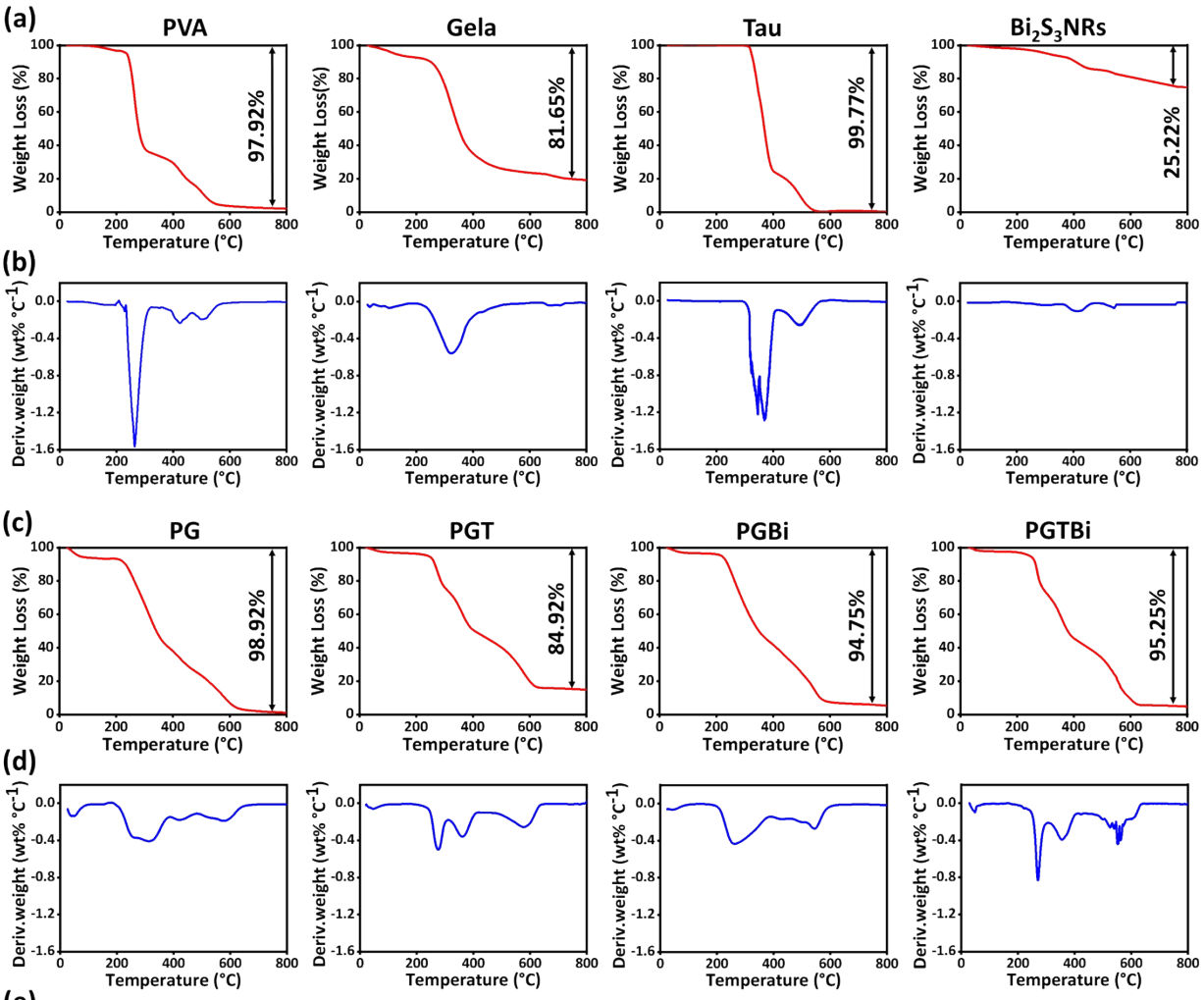

TGA \ Type	PVA	Gela	Tau	Bi_2S_3 NRs	PG	PGT	PGBi	PGTBi
$T_{10\%}$ (°C)	246.12	251.22	329.34	407.57	232.92	265.7	240.15	264.99
$T_{50\%}$ (°C)	278.35	349.31	368.21	---	341.39	406.53	349.85	378.33
Residue at 800 °C	2.08 %	19.20 %	0.23 %	74.78	1.08 %	15.07	5.25 %	4.75 %

Fig. S5. (a) TGA and (b) DTG thermograms of pure materials. (c) TGA and (d) DTG thermograms of PG, PGT, PGBi, and PGTBi nanofiber scaffolds. (e) T 10% and T 50% are the temperatures required to decompose 10% and 50% of each sample, and the residual weight at 800 °C recovered from TGA.

2.6. *In vitro* Insertion of MN Patches

Fig. S6 shows images of Parafilm M® layers inserted with MN patches by hand and the profile of the percentage of holes created and penetration depth. The results show that the MN patches completely pierced the first four layers and reached the seventh layer, and the penetration depth is approximately 762 µm.

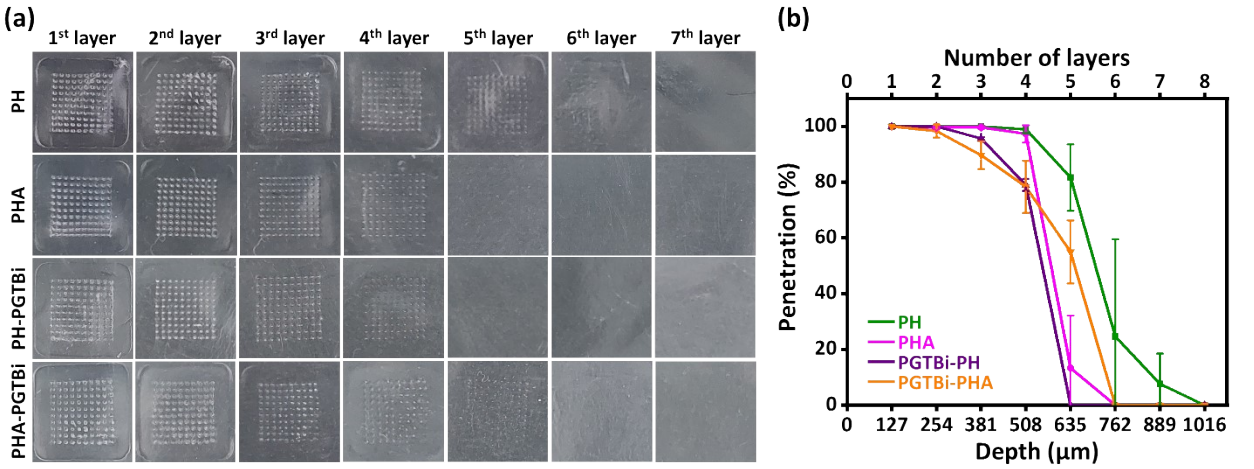

Fig. S6. (a) Images of the first to seventh layers of Parafilm M® after insertion of MN patches with the hand. (b) Linear curve representative of the percentage of holes created per Parafilm M® layer, the number of Parafilm M® layers inserted, and the approximate depth of insertion by MN patches. Data are presented as mean ± SD (N=3).

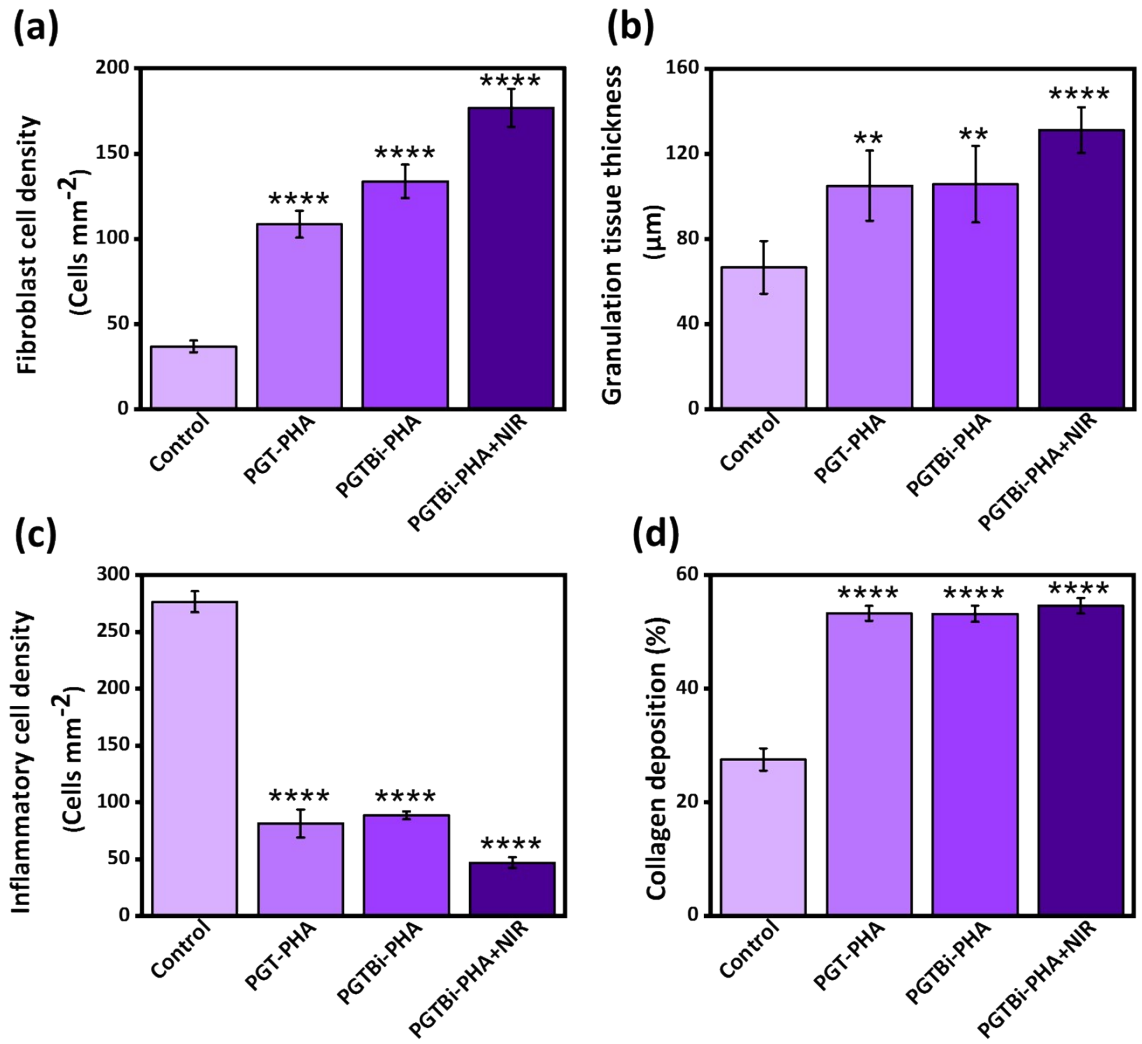

Fig. S7. (a) Quantitative analysis of fibroblast cell density of control, PGT-PHA, PGTBi-PHA and PGTBi-PHA+NIR-treated groups in the full-thickness cutaneous wound model in rats at day 14 obtained from H&E-stained tissues. (b) Quantitative analysis of granulation tissue thickness of control, PGT-PHA, PGTBi-PHA and PGTBi-PHA+NIR-treated groups in the full-thickness cutaneous wound model in rats at day 14 obtained from H&E-stained tissues. (c) Quantitative analysis of inflammatory cell density of control, PGT-PHA, PGTBi-PHA and PGTBi-PHA+NIR-treated groups in the full-thickness cutaneous wound model in rats at day 14 obtained from H&E -stained tissues. (d) Quantitative analysis of collagen deposition of control, PGT-PHA, PGTBi-PHA and PGTBi-PHA+NIR-treated groups in the full-thickness cutaneous wound model in rats at

day 14 obtained from Masson's trichrome-stained tissues. Data are presented as mean ± SD (N = 3), The statistical analysis was performed using One-way ANOVA (**$p < 0.01$, ****$p < 0.0001$ vs. control group).

Reference

1. K. Kavi Rasu, D. Vishnushankar and V. Veeravazhuthi, *Advanced Materials Research*, 2013, **678**, 248-252.
2. S. Farzamfar, M. Naseri-Nosar, H. Samadian, S. Mahakizadeh, R. Tajerian, M. Rahmati, A. Vaez and M. Salehi, *Journal of Bioactive and Compatible Polymers*, 2018, **33**, 282-294.
3. S. Ashkani-Esfahani, F. Zarifi, Q. Asgari, A. Z. Samadnejad, S. Rafiee and A. Noorafshan, *Advanced biomedical research*, 2014, **3**, 204.
4. B. Z. Chen, L. Q. Zhang, Y. Y. Xia, X. P. Zhang and X. D. Guo, *Science Advances*, 2020, **6**, eaba7260.
5. L. Zhao, L. K. Vora, S. A. Kelly, L. Li, E. Larraneta, H. O. McCarthy and R. F. Donnelly, *Journal of Controlled Release*, 2023, **356**, 196-204.
6. A. A. Albadr, I. A. Tekko, L. K. Vora, A. A. Ali, G. Laverty, R. F. Donnelly and R. R. S. Thakur, *Drug Delivery and Translational Research*, 2022, 1-13.
7. S. Shojaie, M. Rostamian, A. Samadi, M. A. S. Alvani, H. A. Khonakdar, V. Goodarzi, R. Zarrintaj, M. Servatan, A. Asefnejad and N. Baheiraei, *Polymers for Advanced Technologies*, 2019, **30**, 1473-1483.
8. R. Rodríguez-Rodríguez, Z. García-Carvajal, I. Jiménez-Palomar, J. Jiménez-Avalos and H. Espinosa-Andrews, *Journal of Applied Polymer Science*, 2019, **136**, 47149.
9. F. N. Parın, Ç. İ. Aydemir, G. Taner and K. Yıldırım, 2020.